JOURNAL OF PROPULSION AND POWER
Vol. 23, No. 5, September–October 2007

Technical Notes

TECHNICAL NOTES are short manuscripts describing new developments or important results of a preliminary nature. These Notes should not exceed 2500 words (where a figure or table counts as 200 words). Following informal review by the Editors, they may be published within a few months of the date of receipt. Style requirements are the same as for regular contributions (see inside back cover).

Airframe-Configuration Effect on Condition of Airflow to Engine in Hypersonic Flow

Takeshi Kanda,* Kanenori Kato,† Masatoshi Kodera,‡
Kenji Kudo,§ and Atsuo Murakami§
Japan Aerospace Exploration Agency,
1 Koganesawa, Kimigaya, Kakuda, Miyagi 981-1525, Japan

DOI: 10.2514/1.29815

Introduction

AEROSPACE planes for a future system of transportation to a low Earth orbit are now under investigation. The scramjet engine and the combined cycle engine have been studied for two-stage-to-orbit or single-stage-to-orbit planes. During flight in the supersonic and hypersonic regions, the windward surface of the vehicle precompresses air into the engine. The engine thrust is approximately proportional to the mass flow rate of the captured air.

Many kinds of airframe configurations of the aerospace plane have been reported, and aerodynamic characteristics of the airframe have been investigated [1–4]. In the present study, the effect of this configuration on the condition of airflow to an engine was experimentally investigated with three typical airframe-configuration models. Their lift and drag by wall pressure integration are also presented.

Test Facility

Tests were conducted at the 1.27 m hypersonic wind tunnel of the Wind Tunnel Technology Center, Japan Aerospace Exploration Agency (JAXA), the Mach number of which is 9.7. The total pressure and the total temperature were 6.0 MPa and 1040 K, respectively. The exit diameter and the wall pressure at the exit of the facility nozzle were 1.27 m and 1.69×10^2 Pa, respectively. The Reynolds number was $3.6 \times 10^6\ \mathrm{m}^{-1}$.

Airframe Model Configuration

Figure 1 shows the experimental models of the forward part of the aerospace plane airframe, from the leading edge to the engine entrance. Pitot pressure rakes were positioned at the engine entrance position. The angle of attack, 0, 2, or 4 deg, was one parameter. Thus, the angles between the airflow and the windward surface of the models were 4, 6, and 8 deg, respectively. The thickness of the leading edge was 0.2 mm.

The width of the leading edge of the models was another parameter. In model A, this width was the same as the width at the position where engine modules are to be attached. Model B had a leading edge of approximately half the width of the body. Model C had an approximately pointed airframe nose. In the models, the imaginary engine entrance was located at 670 mm from the leading edge of the airframe.

The height of imaginary engine modules was 40 mm in the present models, and was expressed as $H0$. According to the two-dimensional shock wave relations, the shock wave from the leading edge was planned to pass 57 mm from the model surface at the angle of attack of 0 deg, and 53 mm at the angle of 4 deg. Pitot pressure was measured in the vertical direction at every 2.5 mm from the model surface to 20 mm and from 50 to 60 mm. Between 20 and 50 mm, the positions were every 5 mm. The measurement positions were nine lateral positions from the center plane: 0, −9, −18, −60, −69, −78, −120, −129, and −138 mm. The pitot tubes were made of Inconel, their outer and inner diameters being 1 and 0.7 mm, respectively. The accuracy of the pitot pressure was 1.5 kPa. Wall pressure of the airframe model was measured at the positions shown in Fig. 1 as intersections. On the leeward surface, wall pressure was measured at the same positions as on the windward surface. The accuracy of the wall pressure was 0.3×10^2 Pa.

The Reynolds number in actual flight will be 6.4×10^7 when the reference length is from the leading edge to the engine. In the present tests, the Reynolds number was 2.4×10^6, lower than the actual value. For transition of the boundary layer, the models were coated with aluminum particles 500–600 μm in diameter, as shown in Fig. 1. According to the schlieren photos, this boundary layer transition was attained only at the 4 deg angle of attack with the coating.

Results and Discussion

Shock Wave Location

Figure 2 shows the location of the shock waves judged from the change of the pitot pressure. In the figure, $H1$ is 1.25 times and $H2$ is 1.5 times as high as $H0$, respectively. The shock wave from the model leading edge passed near the edge of the pitot rake, apart from the calculated position. According to the schlieren photos, this was caused by the rapid growth of the boundary layer in the vicinity of the leading edge.

As the width of the leading edge of the airframe became short, the shock wave passed near the model surface, especially around the sides of the airframe models. The distributions showed that the large width of the leading edge was favorable for precompression. The uniformity of airflow flowing to an engine was largest in model A with the greatest leading-edge width. A similar result was attained by an inviscid computational fluid dynamics calculation [5].

Airflow Rates

Rates of airflow to the engine were calculated with the pitot pressure measured at the imaginary model position. The wall pressure was used in place of static pressure. Figure 3 shows the rates

Presented as Paper 3420 at the 21st AIAA Applied Aerodynamics Conference, Orlando, FL, 23–26 June 2003; received 16 January 2007; revision received 17 April 2007; accepted for publication 21 April 2007.

*Manager, Combined Propulsion Research Group. Senior Member AIAA.
†Senior Researcher, Engine Systems Section, Combined Propulsion Research Group. Member AIAA.
‡Researcher, High Enthalpy Shock Tunnel Section, Combined Propulsion Research Group. Member AIAA.
§Senior Researcher, Engine Systems Section, Combined Propulsion Research Group.

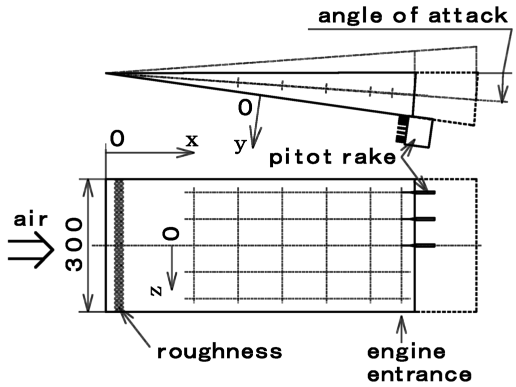

a) Model A

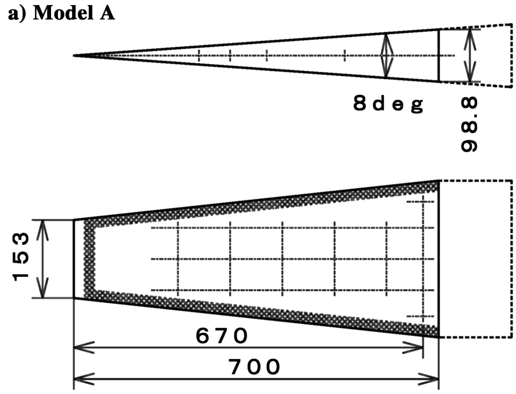

b) Model B

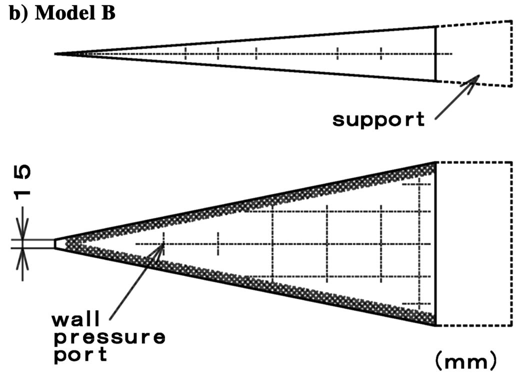

c) Model C

Fig. 1 Aerospace plane forebody models. The shaded area denotes coating of aluminum particles for the boundary-layer transition.

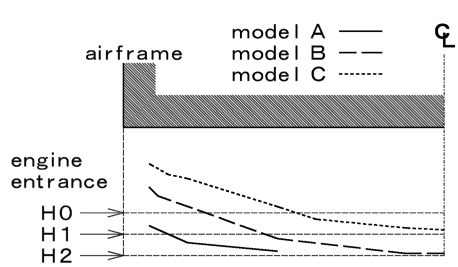

Fig. 2 Locations of shock wave from leading edge at 4 deg angle of attack.

of the three airframe models at the angle of attack of 4 deg. The rates were normalized with mass flux of the core flow ρu_∞ and the projected area at the imaginary engine entrance A, eg.

As the height of the engine increased from $H0$ to $H2$, the ratio of the boundary layer decreased, whereas the ratio of the airflow rate

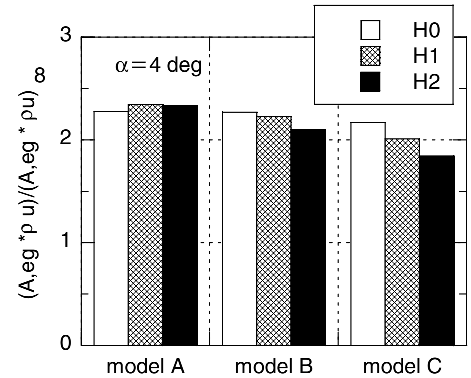

Fig. 3 Rate of airflow into the engine at 4 deg angle of attack.

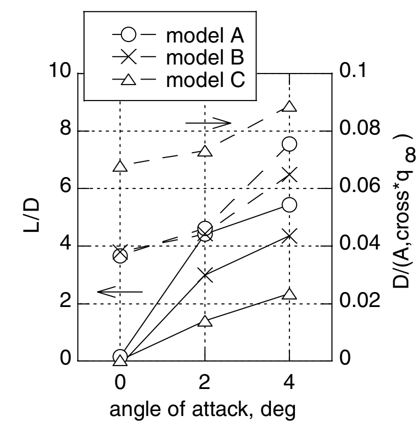

Fig. 4 L/D and pressure drag.

without precompression increased. The decrease of the normalized airflow rate with the increase of the engine height was significant in models B and C. In the models, the ratio of the nonprecompressed airflow rate increased with the increase of the engine height, as shown in Fig. 2. The rate of airflow into an engine was large in the model with a long leading edge.

Pressure Drag and Lift of the Models

By integrating the wall pressure on the model surface, approximate pressure drag and lift of the models could be estimated. Figure 4 shows ratios of lift to drag L/D as solid lines and the drag normalized with the cross section of the airframe model at the engine entrance position (A, cross) and the dynamic pressure of the inflow air q_∞ as broken lines. The integration did not include the base area. The L/D of model A with a rectangular projected area was similar to a previous result [6].

The lift of model A was greater than that of model B, and the lift of model B was greater than that of model C. In model C, the drag was larger than those of the other two models. The difference in the L/Ds was caused by these differences in lift and drag.

The pressure on the side surface remained approximately constant at all three angles of attack. In model B, at the 4 deg angle of attack, the pressure on the side was lower than the pressure on the windward surface. Therefore, the drag of model B became smaller than that of model A. In model C, the side surface had a larger angle to the airflow than the windward surface, and the pressure on the sides was higher than the pressure on the windward surface. Therefore, the drag of model C was greater than those of the other two models.

Conclusions

The effect of the airframe configuration on the condition of airflow to the engine was experimentally investigated with three kinds of forebody models in Mach 9.7 flow. The present study clarified the following points:

1) The uniformity of airflow to an engine was greatest in model A with the longest width at its leading edge.

2) The airflow rate to the engine was large with large width of the leading edge of the airframe. This feature became significant in an engine with large height at the entrance.

3) The ratio of lift to drag was large in the model with a long leading edge.

Acknowledgments

The authors appreciate the kindness of A. Murakami and Y. Watanabe of Japan Aerospace Exploration Agency, and T. Yamaji, a graduate student of Tokyo University of Science and currently a research engineer of Mitsubishi Heavy Industry, Ltd., for acquisition of pressure data. The authors also wish to thank the staff of the Hypersonic Wind Tunnel Section of Japan Aerospace Exploration Agency for conducting the experiments.

References

[1] Ide, H., Armstrong, J., Szema, K. Y., and Haney, J., "Hypersonic Vehicle Forebody Design Studies," AIAA Paper 89-2182-CP, 1989.

[2] Berens, T. M., and Bissinger, N. C., "Forebody Precompression Effects and Inlet Entry Conditions for Hypersonic Vehicles," *Journal of Spacecraft and Rockets*, Vol. 35, No. 1, 1998, pp. 30–36.

[3] Bertin, J. J., Towne, M. C., Malan, M. A., Kreins, A. F., Zuber, M. E., and Parks, M. B., "Viscous/Inviscid Interactions of the Forebody Flowfield of an Airbreathing Hypersonic Vehicle," *Journal of Spacecraft and Rockets*, Vol. 35, No. 4, 1998, pp. 442–449.

[4] Goonko, Y. P., and Mazhul, I. I., "Some Factors of Hypersonic Inlet/Airplane Interactions," *Journal of Aircraft*, Vol. 39, No. 1, 2002, pp. 37–50.

[5] Kodera, M., Kanda, T., and Tani, K., "Effect of Airframe Geometry on Thrust Performance of Aerospace Plane," AIAA Paper 2000-3342, July 2000.

[6] Hankey, W. L., and Elliott, G. A., "Hypersonic Lifting Body Optimization," *Journal of Spacecraft and Rockets*, Vol. 5, No. 12, 1968, pp. 1463–1467.

R. Bowersox
Associate Editor